Original Research

Contact by melanoma cells causes malignant transformation of human epithelial-like stem cells via alpha V integrin activation of transforming growth factor β1 signaling

Hongyu Sun[1,2], Kaimeng Hu[1], Minjuan Wu[1], Jun Xiong[1], Li Yuan[3], Ying Tang[4], Yongji Yang[4] and Houqi Liu[1]

[1]Research Center of Developmental Biology and Department of Histology and Embryology, Second Military Medical University, Shanghai 200433; [2]Department of Clinical Laboratory, The No. 60 Hospital of PLA, Dali, Yunnan Province 671003; [3]Department of Nephrology, Changzheng Hospital, Second Military Medical University; [4]Department of Mathematics, Second Military Medical University, Shanghai 200433, P.R. China
Corresponding author: Prof Houqi Liu. Email: houqiliu@163.com

Abstract

The embryonic microenvironment is known to suppress the tumorigenic phenotype of aggressive cancer cells; however, the effects of tumorigenic microenvironments on stem cells have not been sufficiently explored due to the lack of suitable model systems. In order to study the tumorigenic microenviornment, we developed a novel *in vitro* model system for induction of malignant transformation of human epithelial-like stem cells (hEpSCs), involving co-cultivation and close contact of hEpSCs with the A375 melanoma cell line, together with mutagen treatment of hEpSCs with dimethylbenzanthracene (DMBA). Both factors (close contact and mutagen treatment) were required to transform hEpSCs *in vitro* and cause phenotypic changes characteristic of epithelial to mesenchymal transition (EMT), including colony formation, decreased E-cadherin and increased N-cadherin and vimentin expression. Direct contact between tumor cells and hEpSCs treated with DMBA increased integrin alpha V (ITGAV gene) expression and caused local activation of the transforming growth factor (TGF)-β1/Smad signaling pathways in hEpSCs. The novel model system described here is being used to elucidate the microenvironmental factors and biological mechanisms involved in the induction of neoplastic progression in hEpSCs *in vitro* by A375 melanoma cells. A better understanding of the molecular mechanisms by which melanoma cells exert these effects on hEpSCs may open up new avenues for therapeutic and preventive cancer interventions.

Keywords: human epithelial-like stem cells, 3D culture model, epithelial–mesenchymal transition, melanoma formation, TGF-β1 signaling pathway, integrin alpha V

Experimental Biology and Medicine 2011; **236**: 352–365. DOI: 10.1258/ebm.2010.010106

Introduction

The somatic mutation theory of cancer has been the prevailing paradigm in cancer research for decades and states that malignant transformation is the result of accumulation of multiple mutations in normal differentiated cells.[1,2] Recent studies have demonstrated that not all tumor cells have the capacity to perpetuate the tumor,[3–8] and that only a subset of tumor cells with stem cell-like properties, called cancer stem cells (CSCs), are capable of driving tumor initiation, progression and recurrence.[9] The current CSC hypothesis suggests CSCs, which arise from normal stem cells (SCs) by mutation of genes that make the stem cells cancerous, is consistent with the classical model of multistep carcinogenesis,[10] as SCs have longer life spans than their differentiated progeny and could accumulate multiple mutations over many years.[11]

Somatic SCs reside in a specialized physical local known as a 'niche'.[12] The microenvironment in the niche is essential for the maintenance and functioning of normal SCs. According to the CSC hypothesis, the first step of tumor formation is the clonal expansion of a mutation-harboring SC within a niche, known as pretumor progression.[11] With additional mutations, these cells may expand beyond the confines of an individual niche into microscopic or larger sized patches/fields.[13] For instance, colon tumors are thought to progress through at least five stages: pretumor patches/fields, hyperplasia, carcinoma *in situ*, invasive carcinoma and metastasis.[14]

The microenvironment has major effects on the development and progression of cancer.[9] In the classical two-stage tumorigenesis model, the microenvironment has been proposed to play a part in the promotion phase.[15] Several groups have demonstrated the involvement of microenvironmental factors in tumor progression and proposed that the microenvironment may promote cancer progression through distinct signaling mechanisms.[16,17] For example, Olumi *et al.*[18] reported that carcinoma-associated fibroblasts can direct tumor progression of initiated prostate epithelial cells by SV40-T.

Recent attention has been given to the interactions between stem cells and melanoma cells. Indeed, the bidirectional microenvironmental communication may be propagated among cells through at least three different mechanisms: direct cell–cell contact, autocrine and paracrine signaling driven by soluble secreted factors, and modeling (or re-modeling) of the extracellular matrix.[19] Postovit and colleagues studied the epigenetic influence of the microenvironment of human embryonic stem cells on the reprogramming of aggressive melanoma cells using an innovative three-dimensional (3D) culture model. They demonstrated redifferentiation of the melanoma cells to a melanocyte-like phenotype after exposure to the microenvironment of human embryonic stem cells.[20] Further studies with this model revealed that the aggressive melanoma-conditioned matrix microenvironment induced transdifferentiation of normal melanocytes into melanoma-like cells exhibiting a vasculogenic phenotype.[21] These studies demonstrated that the embryonic microenvironment may have a significant influence on the phenotypic characteristics of aggressive cancer cells; however, the effects of a tumorigenic microenvironment on normal stem cells have not been sufficiently explored.

In this study, we established a novel *in vitro* 3D co-culture model system in order to induce malignant transformation of human epithelial-like stem cells (hEpSCs) in a microenvironment created by the A375 melanoma cell line. Using a two-step protocol (exposure to the mutagen 7,12-dimethylbenz[a]anthracene [DMBA] and subsequent direct contact with A375 melanoma cells), we showed that hEpSCs could be converted to melanoma cells via a mechanism involving integrin alpha V-mediated activation of transforming growth factor (TGF)-β1 signaling.

Materials and methods

Cell cultures

hEpSCs were isolated from the dermis of aborted human fetuses as described previously,[22] which were aged about 20 weeks, collected from a local hospital and approved by the Chinese Ethical Committee of the Institute of Zoology. hEpSCs were cultured on a mitomycin C-treated NIH3T3 feeder layer in the medium using the method as previously reported.[23] The medium was made up of the following: three parts of Dulbecco's modified Eagle's medium plus one part of Ham's F-12 medium containing 10% fetal calf serum (Gibco, New York, NY, USA), 20 ng/mL epidermal growth factor (Sigma, St Louis, MO, USA), 5 mg/mL transferring (Sigma), $1.8 \times 10-4$ mol/L adenine (Amresco, Solon, OH, USA), 5 mg/mL insulin (Sigma), 10–10 mol/L cholera toxin (Sigma) and 0.4 mg/mL hydrocortisone (Sigma). The cultures were grown in a humidified 5% CO_2 atmosphere at 37°C and the medium was changed every two days. hEpSCs were passaged at 80% confluence after removing the feeder cells with 0.02% ethylenediaminetetraacetic acid. We examined the high expression of beta1-integrin and keratin 19 (data not shown) using immunofluorescence, which were previously reported to be important markers for epidermal stem cells. A375 cells (Cell Bank, Chinese Academy of Sciences, Shanghai, China) were cultured in Dulbecco's modified Eagle's medium supplemented with 10% fetal calf serum (FCS; Gibco), 2 mmol/L L-glutamine, 100 U/mL penicillin and 100 μg/mL streptomycin at 37°C with 5% CO_2.

Co-culture model of A375 and hEpSCs or hEpSCs treated with DMBA *in vitro*

In some experiments, hEpSCs were treated with 0.1 μg/mL DMBA (Sigma-Aldrich, St Louis, MO, USA) for 16 h prior to the co-culture with A375 cells. For contact co-culture, A375 cells were first seeded on the bottom of a porous membrane of a cell culture insert (Falcon 6-well cell culture inserts, pore size 0.4 μm; 353090; BD Falcon^{TM}, Micronic, Lelystad, the Netherlands) and cultured with the bottom upwards at 37°C in a 5% CO_2 in air atmosphere for six hours. Then the inserts were transferred to the six-well plates and cultured at 37°C in a 5% CO_2 in air atmosphere for 24 h. hEpSCs or hEpSCs treated with DMBA were seeded on the top sides of the cell culture insert. In the non-contact culture, hEpSCs or hEpSCs treated with DMBA were seeded on the top sides of the cell culture insert whereas the A375 cells were grown at the bottom of the six-well plate with the same method. hEpSCs or hEpSCs treated with DMBA were seeded alone on the top of the porous membrane of the insert as an additional control.

Xenograft tumorigenicity

BALB/c nude mice were maintained in a specific pathogen-free facility. hEpSCs at passage six were treated with 0.1 μg/mL DMBA for 16 h, and then co-cultured with A375 cells for seven days. hEpSCs with 1×10^6 cells/mL in the experiment groups were suspended in 100 μL cold phosphate-buffered saline (PBS) before implantation and inoculated subcutaneously into the right posterior flank of six-week-old immunodeficient mice as previously described.[21] Six mice were used for each condition. Tumors were measured with a digital caliper every two or three days to estimate tumor volume until the xenograft reached 1–1.5 cm or termination of the study. Tumor volume was calculated with the formula $4/3\prod \times (d/D)\ 2 \times D/2$, where d is the minor tumor axis and D is the major tumor axis. All animal procedures were approved by the Ethical Commission of the Second Military Medical University (Shanghai, China).

Anchorage-independent colony formation assay

After seven-day co-culture, we first wiped A375 cells on the bottom of porous membrane of the cell culture using a cotton swab, and digested hEpSCs treated with DMBA on the top sides of the cell culture insert in the control, no-contact and contact groups with 0.25% trypsin. Then, hEpSCs treated with DMBA in the three groups at day 7 were separately plated into soft agar (Wako, Osaka, Japan) in a 60-mm culture dishes (Geriner) according to 1000 cells per dish. The cells were suspended in 3 mL of 0.35% agar supplemented with the culture medium. The cell suspension was layered over the bottom layer of 3 mL of 0.6% agar. Colonies >50 mm in diameter were counted in triplicate dishes at day 21 of culture and the average number of three culture dishes was recognized as the means.

Proliferation curve *in vitro*

Cell proliferation and cell death were assessed using Trypan blue staining. hEpSCs treated with DMBA in the control, no-contact and contact groups as the above isolated method were plated into a 24-well plastic tissue culture plate (Geriner) according to 2×10^4 cells per well. The cultures were grown for seven days. The cells of every three wells were trypsinized for enumerating the number of viable cells separately each day. The cells of each well were enumerated triplicately and the average number of three wells was recognized as the means daily. The growth curves of hEpSCs in the three groups were also displayed as the same process.

Cell migration and invasion assays

hEpSCs treated with DMBA in the three groups for migration were assessed using modified Boyden chambers. The lower surfaces of transwells (8 μm pore size; Costar Corp, Cambridge, MA, USA) were precoated with 1 mg/mL of gelatin for two hours at 37°C. The transwells were then assembled in a 24-well plate (Fisher Scientific Co., Pittsburgh, PA, USA). The lower chamber was filled with serum-free medium. Monolayer cells were collected by trypsinization, washed and resuspended in serum-free medium at a concentration of 5×10^5 cells/mL; 5×104 cells were then inoculated onto the upper side of each modified Boyden chamber. The plates were placed at 37°C in 5% CO_2/95% air and migration was left to proceed for 16 h. Cells at 37°C that had migrated to the lower surfaces of the filters were fixed with 10% formalin phosphate and stained with 0.1% crystal violet–20% methanol (v/v). Images of at least five random fields per filter were digitized (×100 magnification). The average number of migrating cells per field was quantified using Northern Eclipse software (Empix Imaging Inc, Mississauga, ON, Canada). Migration data are expressed as a mean value derived from at least three independent experiments.

Western blot analysis

Expression of E-cadherin was examined using a goat polyclonal antibody against E-cadherin (1:1000 dilution; Santa Cruz Biotechnology; Santa Cruz, CA, USA). Expression of ITGAV (integrin alpha V) was determined using mouse monoclonal antibodies (1:1000 dilution; Santa Cruz Biotechnology). Phosphorylated Smad2 was determined using a monoclonal mouse anti-human antibody (Santa Cruz Biotechnology). Samples were lysed at 0°C using a lysis buffer containing: 50 mmol/L Hepes (pH 7.5), 150 mmol/L NaCl, 1.5 mmol/L $MgCl_2$, 1 mmol/L EGTA, 10% glycerol, 1% Triton X-100, 1 μg/mL aprotinin, 1 μg/mL leupeptin, 1 mmol/L phenylmethylsulfonyl fluoride and 0.1 mmol/L sodium orthovanadate. Supernatant containing 40 μg protein was boiled for five minutes in a sodium dodecyl sulfate (SDS) sample buffer and subject to 10% SDS electrophoresis. Proteins were transferred on to a nitrocellulose membrane by semi-dry transfer at 200 mA for two hours and probed with a primary antibody. Primary antibodies were detected by horseradish peroxidase-conjugated anti-IgG and visualized using an ECL system (Amersham, Arlington Heights, IL, USA).

Histology and immunohistochemistry

After the mice were sacrificed, the nodules were immediately removed and fixed in 10% phosphate-buffered formalin, and then embedded in paraffin. Four-micron-thick sections were prepared and mounted on poly-L-lysine-coated slides (Sigma), and stained with hematoxylin & eosin (HE). To confirm the human origin of the tumor cells, we performed immunohistochemistry staining of human leukocyte antigen (HLA) class I using a monoclonal mouse anti-human HLA class I antibody (1:100 dilution; Sigma). ChemMate Detection Kit (peroxidase/3,3 V-diaminobenzidine, rabbit/mouse; DakoCytomation, Carpinteria, CA, USA) was used for immunodetection. To confirm the characteristics of the tumor, cytoplasmic staining with a monoclonal mouse anti-human Melan-A antibody (A103, 1:100 dilution; Neomarkers, Fremont, CA, USA) for the detection of malignant melanoma in the contact groups was performed. Slides were then incubated with a donkey anti-mouse Ig-Cy3 (1:200 dilution; Boster Biotechnologies Inc, Beijing, China). For negative control, isotype controls were used in all the immunstaining experiments. Slides were observed under an Olympus FluoView Confocal Laser Scanning Microscope (CLSM) with Ar and He/Ne lasers.

Fontana–Masson staining

Deparaffined slides were fixed in formalin, and treated as in the following steps: 3.3% silver amine solution for 90 min at 60°C, 0.2% gold chloride for 10 min at room temperature, 5% sodium thiosulfate for five minutes and counterstaining with nuclear fast red (Sigma).

Immunostaining

We carefully wiped A375 cells on the bottom of the porous membrane of the cell culture using a cotton swab, digested hEpSCs on the top sides of the cell culture insert with 0.25% trypsin and seeded these cells in the three groups separately

on the slides. hEpSCs were incubated with one of the following primary antibodies: N-cadherin, Vimentin (goat polyclonal antibody, 1:100 dilution; Santa Cruz Biotechnology), ITGAV and p-Smad2 (monoclonal mouse antihuman antibody, 1:100 dilution; Santa Cruz Biotechnology). Cells were then incubated with a donkey anti-goat Ig-Cy3, mouse anti-rabbit Ig-Cy3 and goat anti-mouse Ig-FITC (1:200 dilution; Boster Biotechnologies Inc). For negative control, primary antibodies were omitted. Cells were observed under an Olympus FluoView CLSM with Ar and He/Ne lasers, or Leica LSM TCS SP2 AOBS CLSM with Ar, He/Ne and blue diode lasers.

Flow cytometry analysis

hEpSCs were detached with 0.25% trypsin. Before staining, cells were washed twice with PBS. Then, 1×10^5 cells per sample were incubated for 30 min at 4°C with one of the following primary antibodies: N-cadherin and Vimentin, at varying concentrations. After the incubation with primary antibody, cells were washed twice in PBS containing 1% bovine serum albumin (PBS-BSA) and re-suspended in 400 μL PBS-BSA containing 4 μg secondary antibodies. After 30 min incubation at 4°C, cells were washed twice in PBS-BSA and re-suspended in 200 μL PBS. An isotypic control (IgG2a, Beckman-Coulter, Fullerton, CA, USA) was used to determine non-specific binding. Fluorescence of cell was analyzed with a FACS Vantage flow cytometer (Becton-Dickinson, Grenoble, France). A total of 10^5 cells of each sample were analyzed at a flow rate of 1000 cells/s.

Total RNA isolation and semi-quantitative reverse transcriptase polymerase chain reaction analysis

Total RNA was extracted using the TRIzol reagent (Life Technologies, Gaithersburg, MD, USA). One microgram of total RNA was used for first-strand cDNA synthesis followed by specific gene product amplification with the One-step RT-PCR Kit (Invitrogen, Life Technologies). Primers for ITGAV (forward, 5′-TGAGGATATCACCAACTCCACA-3′; reverse, 5′-GTTGCTAATTCTAGTGGGTCA-3′) and for 18s (forward, 5′-GTAACCCGTTGAACCCCATT-3′; reverse, 5′-CCATCCAATCGTAGTAGCG-3′) were both derived from human sequences. Polymerase chain reaction (PCR) conditions were optimized so that the gene products were examined at the exponential phase of their amplification and the products were resolved on 1.8% agarose gels containing 1 μg/mL of ethidium bromide.

cDNA synthesis and realtime quantitative reverse transcriptase-PCR

Total RNA was extracted from fresh nodules that were formed by hEpSCs treated with DMBA in the contact group in nude mice at different times. For cDNA synthesis, 1 μg total RNA was reverse-transcribed into cDNA using high-capacity cDNA reverse transcription kit (Applied Biosystems, Foster City, CA, USA). Primer sequences for MITF were: CCGTCTCTCACTGGATTGGT, TACTTGGT GGGGTTTTCGAG. Gene expression was quantified by realtime quantitative PCR using iQ SYBR Green Supermix (Bio-Rad Laboratories, Inc, Hercules, CA, USA). DNA amplification was carried out usingIcycler iQ5 (Bio-Rad Laboratories, Inc) and product detection was done by measuring the binding of the fluorescent dye SYBR Green I to double-stranded DNA. All the primer sets were provided by Qiagen (Valencia, CA, USA). The relative quantities of target gene mRNA against an internal control, 18S rRNA, were measured by following a ΔC_T method. An amplification plot that had been the plot of fluorescence signal versus cycle number was drawn. The difference (DCT) between the mean values in the triplicate samples of target gene and those of 18S rRNA were calculated by iQ5 Optical System Software version 2.0 (Bio-Rad) and the relative quantified value was expressed as 2 ΔC_T.

Enzyme-linked immunosorbent assay

The levels of cytokines, growth factors and chemokines (TGF-β1, TGF-β2, matrix metalloproteinase [MMP]-1, MMP-2, MMP-3, GRO and ENA) in the various culture supernatants were measured by the corresponding Quantikine ELISA kit (R&D Systems) according to the manufacturer's protocols.

Knockdown ITGAV by RNAi in hEpSCs

To establish stable expression of small interfering RNA (siRNA) in hEpSCs, we used the siRNA expression vector pGCsilencerTM U6/NEGative vector (Genscript Corp, Piscataway, NJ, USA), which co-expresses green fluorescent protein to allow identification of transfection efficiency. ITGAV specific and non-specific siRNA sequences were synthesized by GeneChem Corp (Shanghai, China) and inserted into the pGCsilencerTM U6/NEGative vector. The targeting sequence of the shRNA was 5′-CAATGAAAGG AGCCACAGATA-3′ (GenBank GI: NM_002210), and confirmed by sequencing. A non-specific siRNA expression vector was also generated for use as a negative control. The plasmid was transfected into hEpSCs by a lipofection method, using Lipofectamine 2000 (Invitrogen) according to the manufacturer's protocol. Stably transfected colonies showing suppression of ITGAV protein were selected after neomycin (Invitrogen) treatment at 200 μg/mL and used for the subsequent experiments. The extent of siRNA-mediated inhibition of ITGAV was evaluated by Western blot analysis with specific antibodies.

Statistical analysis

Experiments were performed in triplicate and results are expressed as mean $\pm$ standard deviation (SD). For the tumor volume assays, data were analyzed using analysis of variance, followed by the Student–Newman–Keuls test for pairwise multiple comparisons. Other data were analyzed using Student's *t*-test. In all experiments, differences were considered statistically significant at $P < 0.05$, and an asterisk (*) identifies such significance in the figures.

Results

hEpSCs formed melanoma *in vivo* when treated with DMBA and then cultured in contact with A375 melanoma cells

hEpSCs at passage six were treated with or without 0.1 μg/mL DMBA for 16 h, and then co-cultured with A375 cells for seven days. Three groups of cultures were studied: (1) contact group, hEpSCs or hEpSCs treated with DMBA + A375 melanoma cells in contact co-culture for seven days by seeding on the bottom and top sides of a porous membrane of a cell culture insert, respectively; (2) no contact group, hEpSCs or hEpSCs treated with DMBA + A375 melanoma cells co-cultured without contact (separated by cell culture insert) but allowing hEpSCs to be exposed to the A375 conditioned media for seven days; and (3) control (control cultures containing hEpSCs or hEpSCs treated with DMBA only for 7 days). To assess the tumorigenesis of hEpSCs or hEpSCs treated with DMBA in the three groups, we established a xenograft model. Fourteen days after receiving hEpSCs or hEpSCs treated with DMBA in the three groups, nodules appeared in nude mice at 14 d and only hEpSCs treated with DMBA in the contact group formed black nodules (Figure 1a) and, therefore, the cells we studied in the following experiments were hEpSCs treated with DMBA. The growth kinetics of hEpSCs treated with DMBA in the contact group xenografts in nude mice ($n = 6$ for each experimental group) showed the proliferous ability of transformed hEpSCs *in vivo*. HE staining of the subcutaneous tissue showed significant differences among the three experimental groups (Figure 1b). Fontana–Masson staining for melanin revealed hyper-pigmentation in the contact group, but not in the other two groups (Figure 1b). However, hEpSCs without treatment with DMBA in the three groups of cultures presented no pigmentation in the contact group (data not shown). HLA-1 immunohistochemistry confirmed the human origin of the cells with hyper-pigmentation (Figure 1b). Cytoplasmic staining with Melan-A by fluorescence microscopy showed the expression of the melanoma antigen in the skin (Figure 1c). Furthermore, quantitative PCR revealed the expression of MITF *in vivo* (Figure 1d). These data preliminarily indicated that transformed hEpSCs were able to form a melanoma-like tumor *in vivo*.

hEpSCs undergo maligant transformation and epithelial–mesenchymal transition when treated with DMBA and then cultured in contact with A375 melanoma cells

Transformed hEpSC colonies were observed at day 7 in hEpSCs treated with DMBA and in direct contact to A375 cells, but not in the non-contact group or in hEpSCs treated with DMBA cultured alone (Figure 2a). The 'pile-up' appearance of hEpSC colonies in the contact group prompted us to examine their anchorage-independent growth in soft agar. We carefully wiped A375 cells on the bottom of the porous membrane of the cell culture using a cotton swab, digested the hEpSCs on the top sides of the cell culture insert with 0.25% trypsin and seeded these cells in the three groups separately in soft agar at the density of 1000 cells per well. After incubation for three weeks, in contrast to the absence of colonies in control group cells, nearly 5% of hEpSCs in the contact group formed large colonies (Figure 2e), indicating that hEpSCs with direct contact to A375 cells had undergone the transformation. Additionally, we monitored the proliferation curve for hEpSCs in the three groups and showed that hEpSCs with direct contact to A375 cells in the contact group had the enhanced proliferation prominently *in vitro* (Figure 2f). Reduction of E-cadherin and concomitant production of N-cadherin are features of epithelial–mesenchymal transition (EMT). In the hEpSCs treated with DMBA and then induced by A375 cells, expression of N-cadherin and Vimentin was significantly increased (Figure 2b), whereas expression of E-cadherin was decreased in the same experimental group (Figure 2d). As is known, down-regulation of E-cadherin is the hallmark molecular change that occurs during EMT. The number of cells positive for N-cadherin and Vimentin in the contact group was significantly increased (Figure 2c). In addition to biochemical changes, a very important aspect of EMT is increased cellular motility. A tumor invasion assay showed migration ability of hEpSCs treated with DMBA and then induced by A375 cells in the contact group was significantly increased compared with the other groups (Figure 2g).

These data indicated that transformed hEpSCs possess mesenchymal characteristics and EMT. However, hEpSCs without DMBA treatment in the three groups of cultures presented no phenotype changes or transformation (data not shown).

The contact of A375 and hEpSCs causes a rise in the levels of TGF-β1 and activation of TGF-β1/Smad signaling pathways

The aforementioned observations indicate that malignant transformation of the hEpSCs required direct contact with melanoma. We speculate that direct contact between melanoma cells and hEpSCs may stimulate certain paracrine signals. To identify these signals, *in vitro* co-cultures of A375 cells and hEpSCs were established and their conditioned media were measured for the levels of various cytokines and growth factors by enzyme-linked immunosorbent assay (ELISA) (Figure 3a). In some cases, certain released factors (for example, MMP-1 or GRO) were higher in the contact group than in the remaining two groups. Notably, TGF-β1 was three-fold higher in the contact culture group than the hEpSCs alone or no-contact co-culture group (Figure 3c), suggesting a synergistic interaction between A375 and hEpSCs. This cooperative induction of TGF-β1 was apparent as early as the third day of co-culture (Figure 3b). To determine whether TGF-β1 signal pathways in hEpSCs are activated in the contact co-culture group, we measured the phospho-Smad2 (p-Smad2), a downstream signal transduction factor of TGF-β1. Importantly, subsequent co-culture of these hEpSCs and cancer cells continued to allow accumulation of p-Smad2 in hEpSCs in the contact co-culture group that were comparable to those observed in the no-contact

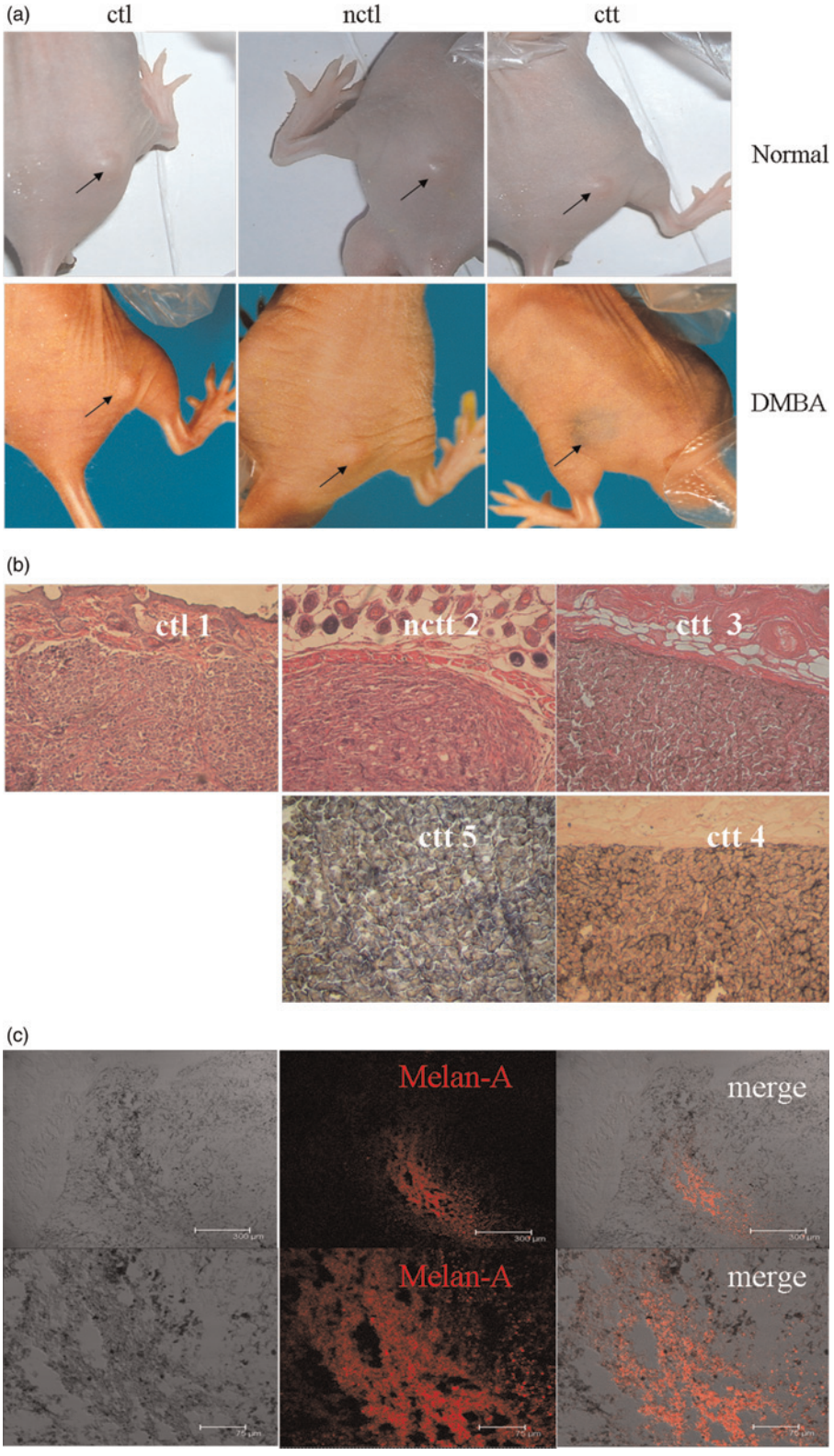

Figure 1 Human epithelial-like stem cells (hEpSCs) formed melanoma *in vivo* when treated with 7,12-dimethylbenz[a]anthracene (DMBA) and then cultured in contact with melanoma cells. (a) *In vivo* nodule formation in nude mice injected with hEpSCs at 14 d when treated with DMBA and then induced by co-culturing with melanoma cells for seven days. Normal: hEpSCs + A375 melanoma cells. DMBA: hEpSCs treated with DMBA + A375 melanoma cells. (b) Epidermis morphology in tumorigenesis model. ctl1/nctt2/ctt3: hematoxylin and eosin staining in control group, no-contact group and the contact group (ctl, nctt, ctt), respectively ($\times$100). ctt4: Fontana–Masson staining in the contact group (ctt) ($\times$200); ctt5: imunohistochemistry alkaline phosphatase staining for human human lelukocyte antigen-1 in the contact group (ctt) ($\times$200). (c) Fluorescence microscopy analysis of cryosections of nodules in the contact group by staining with Melan-A. Top (bar: 300 μm); bottom (bar: 75 μm). (d) Relative gene expression levels of MITF (a melanoma-specific transcription factor) were assessed by quantitative polymerase chain reaction using total RNA extracted from fresh nodules, which were formed by hEpSCs treated with DMBA in the contact group in nude mice at the indicated times (bars: SE; $^{*}P < 0.05$; $^{**}P < 0.01$). RQ, rationality. (A color version of this figure is available in the online journal)

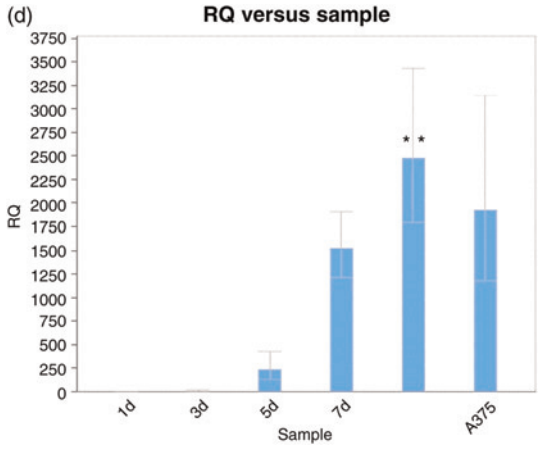

Figure 1 Continued

group and control group (Figure 3d). Meanwhile, immunocytochemistry revealed that p-Smad2 could be detected in the nuclei of 40–60% transformed hEpSCs (Figure 3e), suggesting that direct contact between melanoma cells and hEpSCs activates the TGF-β1/Smad signaling pathways.

Establishment of difference stable ITGAV interference levels of hEpSCs

In our experiments, strong expression of ITGAV protein was detected in hEpSCs after contact co-culture by immunofluorescent microscopy (Figure 4b). To further test the accumulation of ITGAV in the transformed hEpSCs, mRNA expression of ITGAV was assessed by reverse transcriptase (RT)-PCR. Consistent with results of our previous studies, mRNA expression of ITGAV was increased in contact co-culture (Figure 4b). To explore the role of

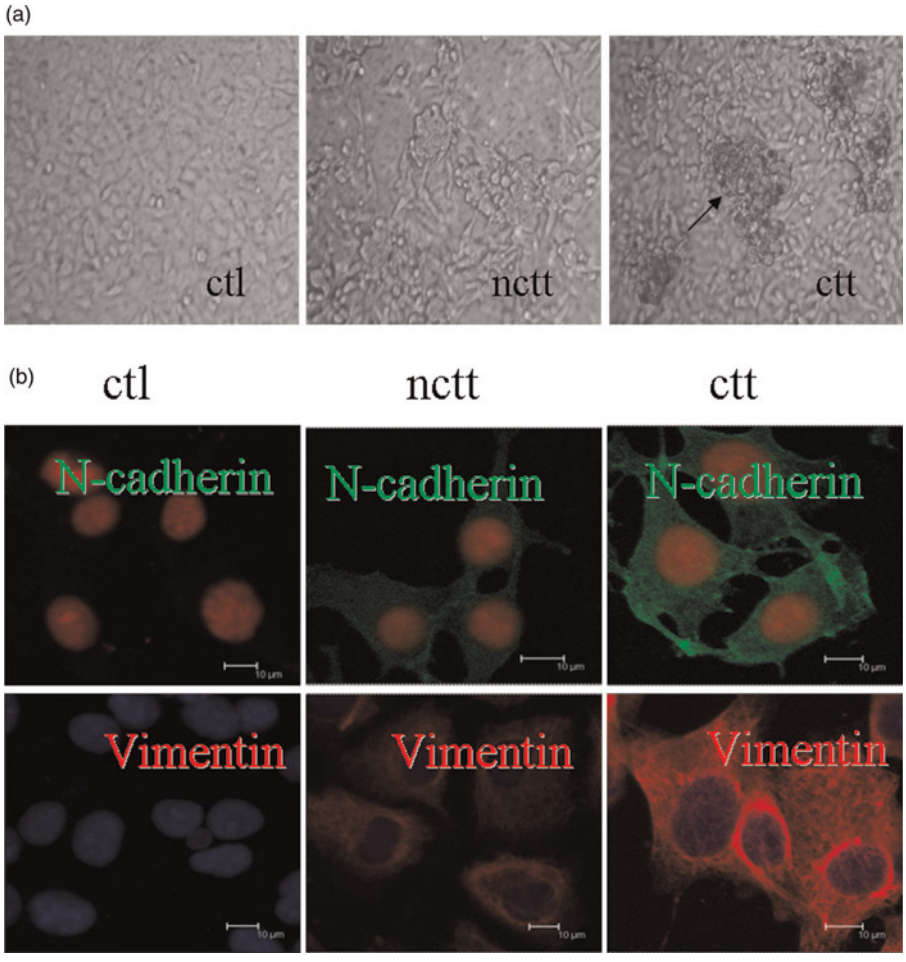

Figure 2 Human epithelial-like stem cells (hEpSCs) undergo epithelial–mesenchymal transition when treated with 7,12-dimethylbenz[a]anthracene (DMBA) and then cultured in contact with melanoma cells. (a) Phase-contrast micrograph of colonies formed by hEpSCs in the contact group (ctt) and not in the no-contact group (nctt) and control groups (ctl) at seven days ($\times$100). (b) Representative confocal images of N-cadherin and Vimentin in hEpSCs, which were treated with DMBA and then induced by co-culturing with A375 cells for seven days. N-cadherin (bar: 10 μm); Vimentin (bar: 30 μm). (c) Proportion of cells positive for N-cadherin and Vimentin in hEpSCs determined by flow cytometry analysis in the three groups (ctl, nctt, ctt). (d) Western blot analysis of E-cadherin in hEpSCs at the indicated time points. (e) hEpSCs originating from the contact group (ctt) can form colonies in soft agar but cells from the other two groups cannot form colonies either ($\times$100). The percentage of anchorage-independent colonies $>$50 mm in diameter after incubation for 21 d. The data represent the mean_standard deviation of triplicate samples. (f) Growth curves of hEpSCs in the three groups are presented. The growth curves were determined in triplicate, and they are representative of three independent experiments. (g) Migration ability of hEpSCs in the three groups is presented. Columns, mean of a representative experiment in which five random fields per filter were counted for each condition (bars: SE; $^{*}P < 0.05$; $^{**}P < 0.01$) (A color version of this figure is available in the online journal)

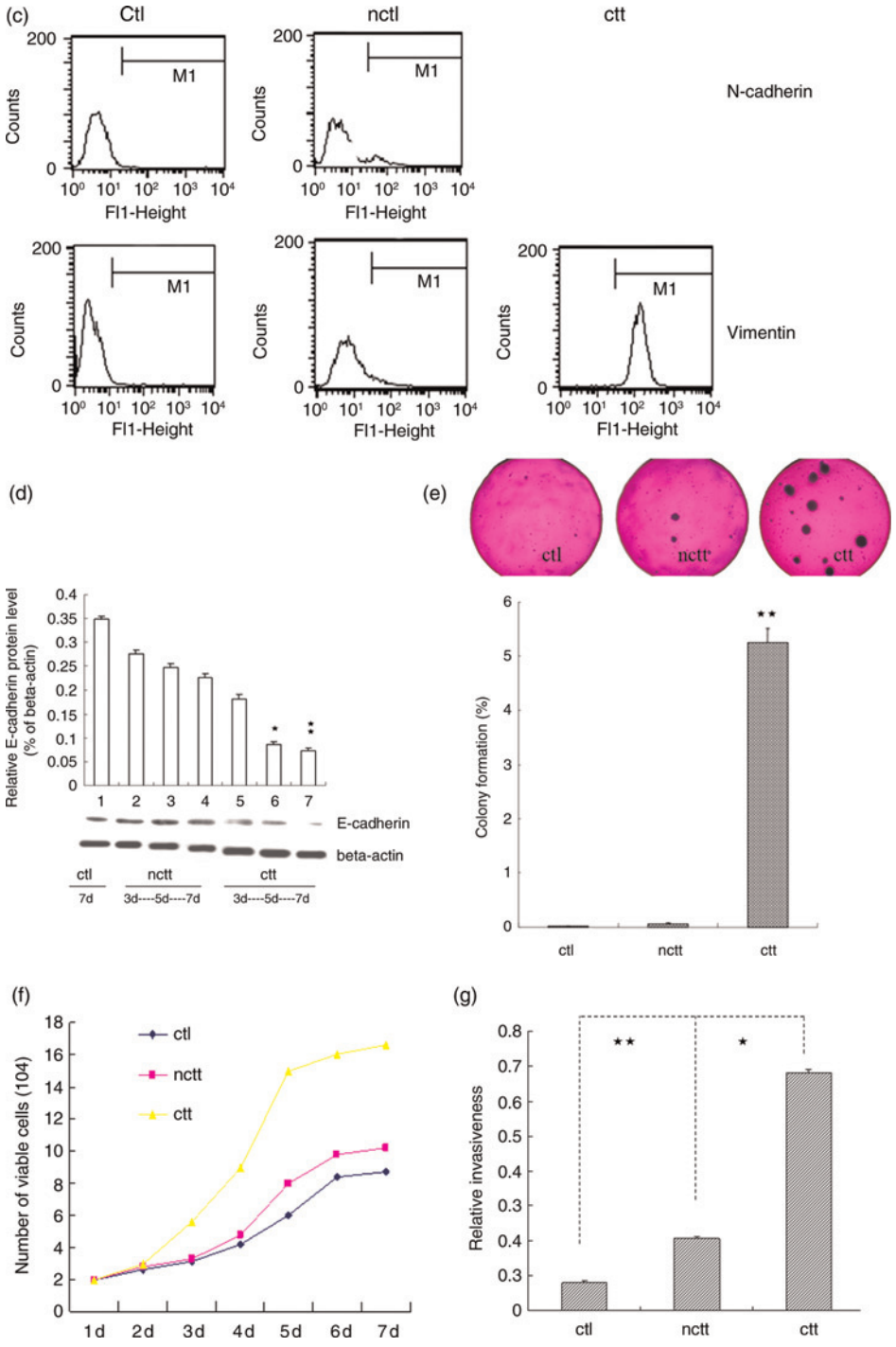

Figure 2 Continued

ITGAV in the process of tumorigenesis, we established stable siRNA expression vectors, pGCsilencerTM U6/NEGative (NCRNAi) and pGCsilencerTM U6/ITGAV (ITGAV RNAi). After transfection of NCRNAi and ITGAV RNAi in cultured human embryonic stem cells (hESCs), colonies (NC, A2, C1, D2 and F4) were selected by neomycin (200 μg/mL). Western blots revealed that ITGAV RNAi treatment decreased total cellular ITGAV protein levels (Figure 4c). Histogram analysis showed the average level of ITGAV interference was 50%, 30%, 70% and 90% (Figure 4d) for A2, C1, D2 and F4, respectively.

ITGAV may be the major tumorigenic molecule and mediate activation of TGF-β1 signaling

To investigate the functional consequences of ITGAV interference in the process of tumorigenesis, the growth kinetics of transformed hEpSCs with ITGAV interference *in vivo* were compared with those of hEpSCs that had been previously co-cultured over four weeks. ITGAV interference inhibited the tumor growth (Figure 4e). More importantly, in the case of ITGAV with interference efficiency of 90% and 70% of hEpSCs, their tumor volume displayed a

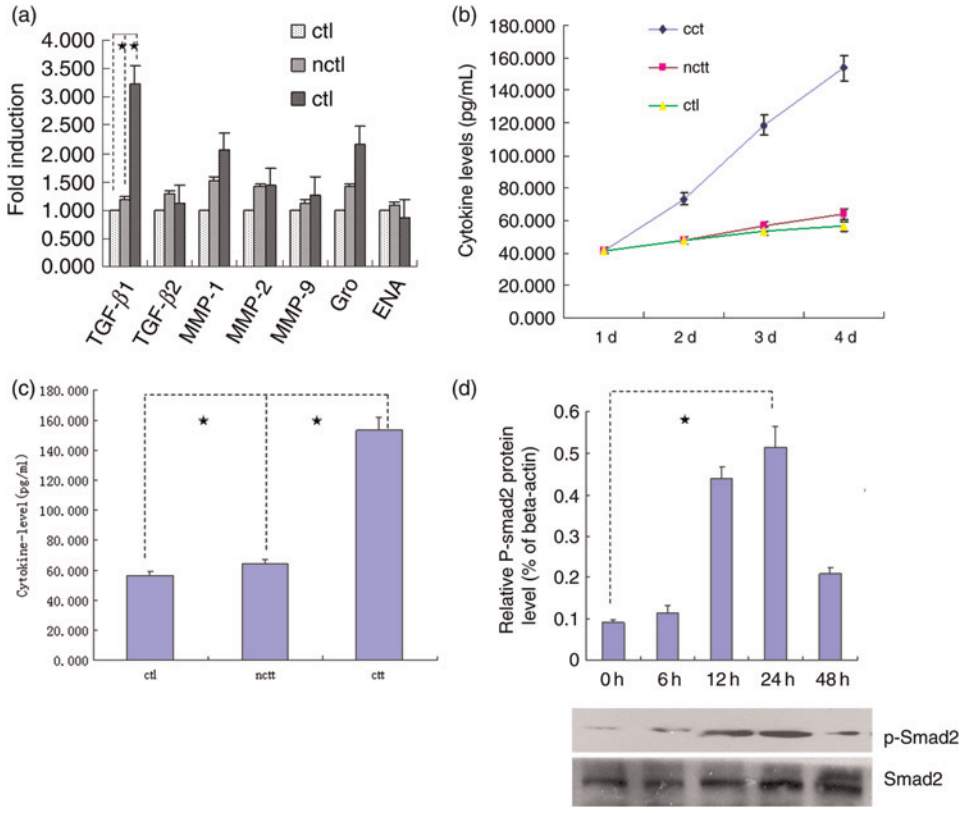

Figure 3 Contact between A375 and human epithelial-like stem cells (hEpSCs) increases the level of transforming growth factor (TGF)-β1 and activates the TGF-β1/Smad signaling pathway. (a) hEpSCs were treated with 7,12-dimethylbenz[a]anthracene (DMBA) and then induced by co-culturing with A375 cells for three days in complete media (contact, no-contact and control groups). The levels of various factors in the cell-free culture supernatants were measured by immunoassay at day 3. Data are expressed as fold induction $\pm$ SD of triplicate experiments (bars: SE; $^{*}P < 0.05$; $^{**}P < 0.01$). (b) TGF-β1 enzyme-linked immunosorbent assay (ELISA) of hEpSC media obtained from the contact, no-contact and control groups at the indicated time points. Data points represent means $\pm$ SD of triplicate experiments (bars: SE). (c) TGF-β1 ELISA of hEpSC media obtained from the contact, no-contact and control groups at the indicated time points. Data are expressed as fold induction $\pm$ SD of triplicate experiments (bars: SE; $^{*}P < 0.05$). (d) Western blots revealed that the expression of P-Smad2 in hEpSCs in the contact group at the indicated time points (bars: SE; $^{*}P < 0.05$). (e) Representative confocal images of p-Smad2 in hEpSCs in the control, no-contact and contact group at three days (bar: 8 μm) (A color version of this figure is available in the online journal)

significant decrease (Figure 4f) by statistical analysis of Figure 4e. These data suggested that ITGAV may contribute to the tumorigenesis.

Since ITGAV and TGF-β1 were involved in the transformation of hEpSCs, we next set out to resolve the relationship between ITGAV and TGF-β1. We measured the levels of TGF-β1 in the media of hEpSCs after stable knockdown of 90% ITGAV. ELISA analysis revealed that stable knockdown of 90% ITGAV did not result in accumulated levels of TGF-β1 in the contact groups (Figure 4g). Western blots of p-Smad2 in hEpSCs after the difference knockdown ITGAV levels in contact co-culture group at three days also showed a weakening of TGF-β1 signaling (Figure 4h). Taken together, these observations suggested that ITGAV mediate the local activation of TGF-β1/Smad signaling pathways.

Discussion

Results from the current study demonstrated that hEpSCs may undergo neoplastic transformation when first treated with the mutagen DMBA and then cultured in contact with melanoma cells. This finding is consistent with the recent notion that microenvironment plays a pivotal role in the development and progression of cancer.[9] Interestingly, Seftor found that the melanoma microenvironment could cause epigenetic transdifferentiation of normal melanocytes to melanoma-like cells, suggesting that normal cells could be re-programmed by inductive cues in the tumor cell microenvironment.[21,24] Melanocytes are not the only cell type susceptible to this kind of epigenetic modulation by a cancerous microenvironment. When hESCs are cultured on a 3D matrix conditioned by aggressive melanoma cells for three days, hESCs exhibit a vasculogenic and mesenchymal-like phenotype following exposure to the microenvironment of metastatic melanoma cells.[19] Malignant transformation of the hEpSCs required exposure to DMBA as well as contact with melanoma. We speculate that DMBA causes permanent gene damage (e.g. mutations in H-ras oncogene), which in turn allows for autonomous growth, and the melanoma microenvironment could function as a classic tumor promoter or co-carcinogen. In addition, it is known that melanomas arise from melanocytes, which originate from the neural crest. However, in our study, hEpSCs formed melanoma-like cells when first treated with the mutagen DMBA and then cultured in contact with melanoma cells. It may be possible that

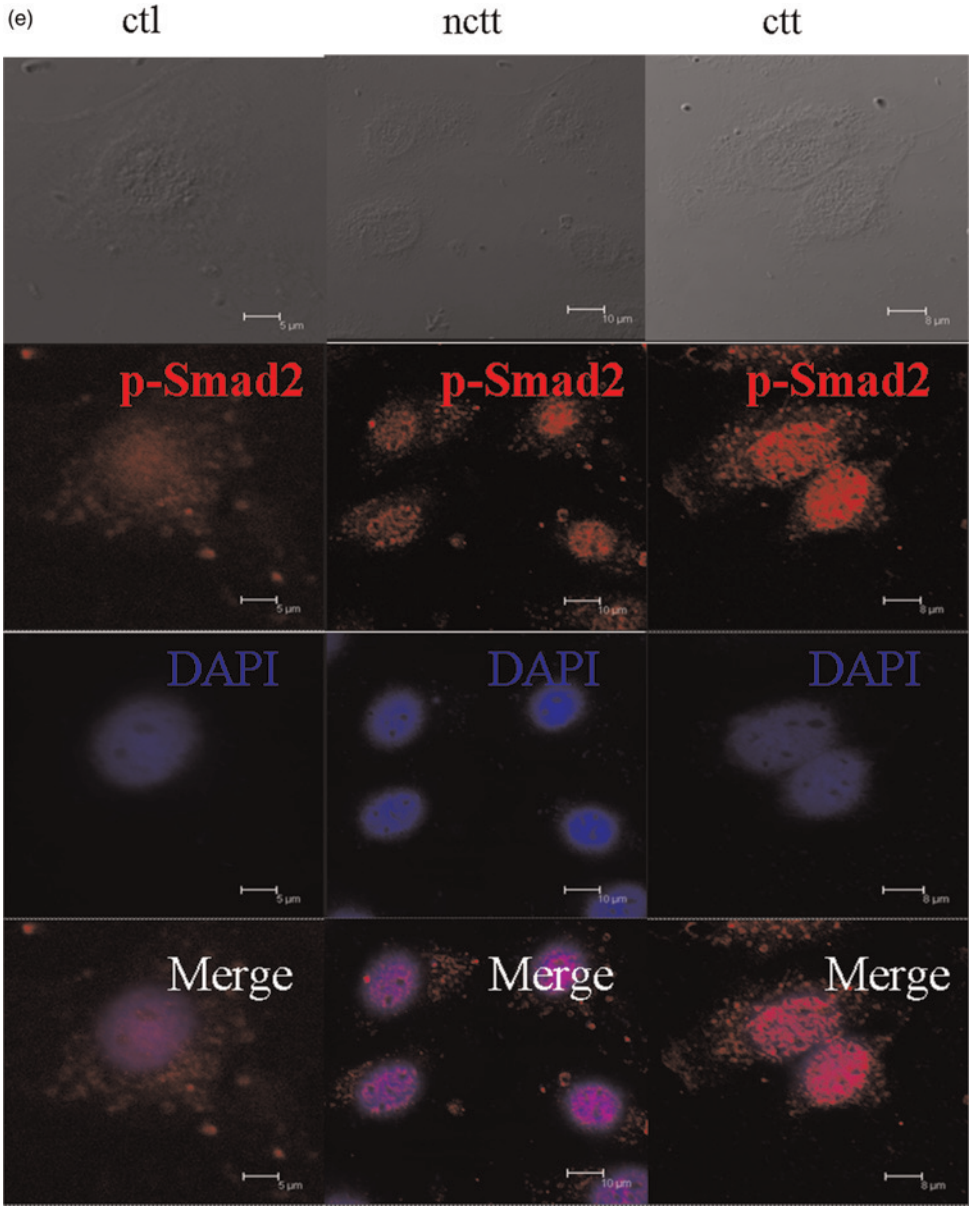

Figure 3 Continued

hEpSCs are derived from the skin of young fetuses and have the capacity of pluripotentiality because we replaced hEpSCs with HaCaT (an immortalized human keratinocyte line) and did not repeat the experiments. We speculate that these fetal precursors are likely proliferating more rapidly than adult cells.

EMT is a remarkable example of cellular plasticity and is pivotal in cancer progression. Reduction of E-cadherin and concomitant production of N-cadherin are characteristic features of EMT.[25,26] During EMT, epithelial cell–cell contact decreases. Cytoskeletal components are down-regulated; mesenchymal markers such as smooth muscle actin and Vimentin are up-regulated.[27,28] In addition to maintaining the epithelial phenotype, expression of N-cadherin is necessary and sufficient to promote EMT and cell motility.[29] We found convincing evidence for EMT in hEpSCs in contact with melanoma cells: expression of mesenchymal markers (N-cadherin, Vimentin) and decreased expression of E-cadherin. Furthermore, analysis of cell proliferation and anchorage independence (soft agar growth) showed hEpSCs underwent neoplastic transformation when first treated with the mutagen DMBA and then cultured in contact with melanoma cells.

EMT can be induced in the tumor microenvironment and can be regulated by the TGF-β signaling pathway.[30–32] The TGF-β1 cytokine is a pleiotropic growth factor that can regulate cell proliferation, differentiation and immune responses.[33,34] Although TGF-β is recognized as an inhibitor of normal epithelial cell proliferation and an early-stage tumor suppressor, tumor cells often acquire resistance to the growth-suppressive activities of TGF-β1 during tumor progression.[35,36] In some tumors, TGF-β1 expression and activity has been implicated in promoting survival, progression and metastases.[37–39] This is

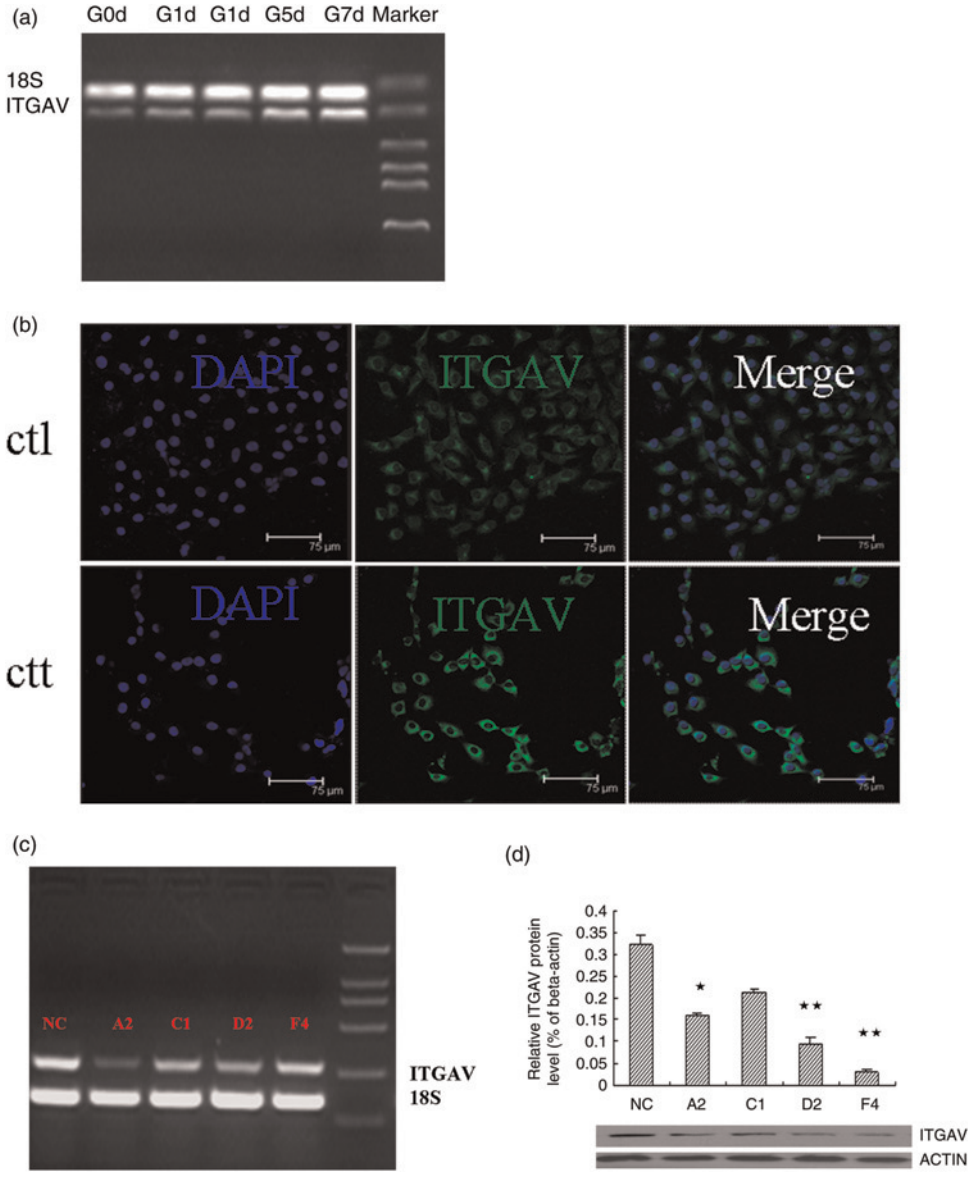

Figure 4 Establishment of different stable ITGAV (integrin alpha V) interference levels of human epithelial-like stem cells (hEpSCs). (a) Reverse transcriptase-polymerase chain reaction (RT-PCR) analysis of ITGAV in hEpSCs in the contact group (ctt) at the indicated time points. 18s rRNA was amplified to confirm that equal amounts of total mRNA were used for each sample. (b) The expression levels of ITGAV on the surface and cytoplasm of hEpSCs in the contact group (ctt) and in the control group (ctl) were tested by immunofluorescence analysis. (c) RT-PCR revealed that the expression of ITGAV protein in cultured hEpSCs infected with non-target control RNAi (NCRNAi) and ITGAV RNAi. Actin is shown as the control for equal protein loading. NC, A2, C1, D2 and F4 were the five colonies selected, respectively. (d) Western blots revealed the expression of ITGAV protein in selected hEpSC NC, A2, C1, D2 and F4 colonies. Actin is shown as the control for equal protein loading. Histograms represent the average level of ITGAV knockdown in the hEpSCs (columns: mean of two independent experiments done in quadruplicate; bars: SE). Values were normalized to those of actin protein in each case. (e) Growth curves of hEpSCs treated with 7,12-dimethylbenz[a]anthracene and then induced by co-culturing with A375 cells for seven days in the contact group xenografts in nude mice ($n = 6$ for each experimental group). Blue, control small interfering RNA (siRNA)-treated hEpSCs (G-RNAiCtl); red, siRNAC1-treated hEpSCs (G-RNAiC1); yellow, siRNAD2-treated HESCs (G-RNAiD2); bluish-green, siRNAF4-treated hEpSCs (G-RNAiF4) (bars: SE). (f) Tumor volumes which come from Figure 4E (mean $\pm$ SEM, $n = 6$) were taken at four weeks. Data shown are representative of triplicate experiments (bars: SE; $^{*}P < 0.05$; $^{**}P < 0.01$). (g) Left: transforming growth factor (TGF)-β1 enzyme-linked immunosorbent assay (ELISA) on hEpSC media after stable knockdown of ITGAV by 90% in the contact, no-contact and control groups at the indicated time points. Data points represent the mean $\pm$ SD of triplicates (bars: SE). Right: TGF-β1 ELISA on hEpSC media after stable knockdown of ITGAV by 90% in the contact, no-contact and control groups (ctl, nctt, ctt) at day 3. Data points represent mean $\pm$ SD of triplicates (bars: SED). (h) Representative Western blots of p-Smad2 in hEpSCs after the ITGAV knockdown levels in the contact co-culture group (ctt) at three days. Histograms represent the average level of p-Smad2 in the hEpSCs after ITGAV knockdown in the contact co-culture group (ctt) at three days. (Columns: mean of two independent experiments done in quadruplicate; bars: SE; $^{*}P < 0.05$; $^{**}P < 0.01$.) Values were normalized to those of Smad2 protein in each case (A color version of this figure is available in the online journal)

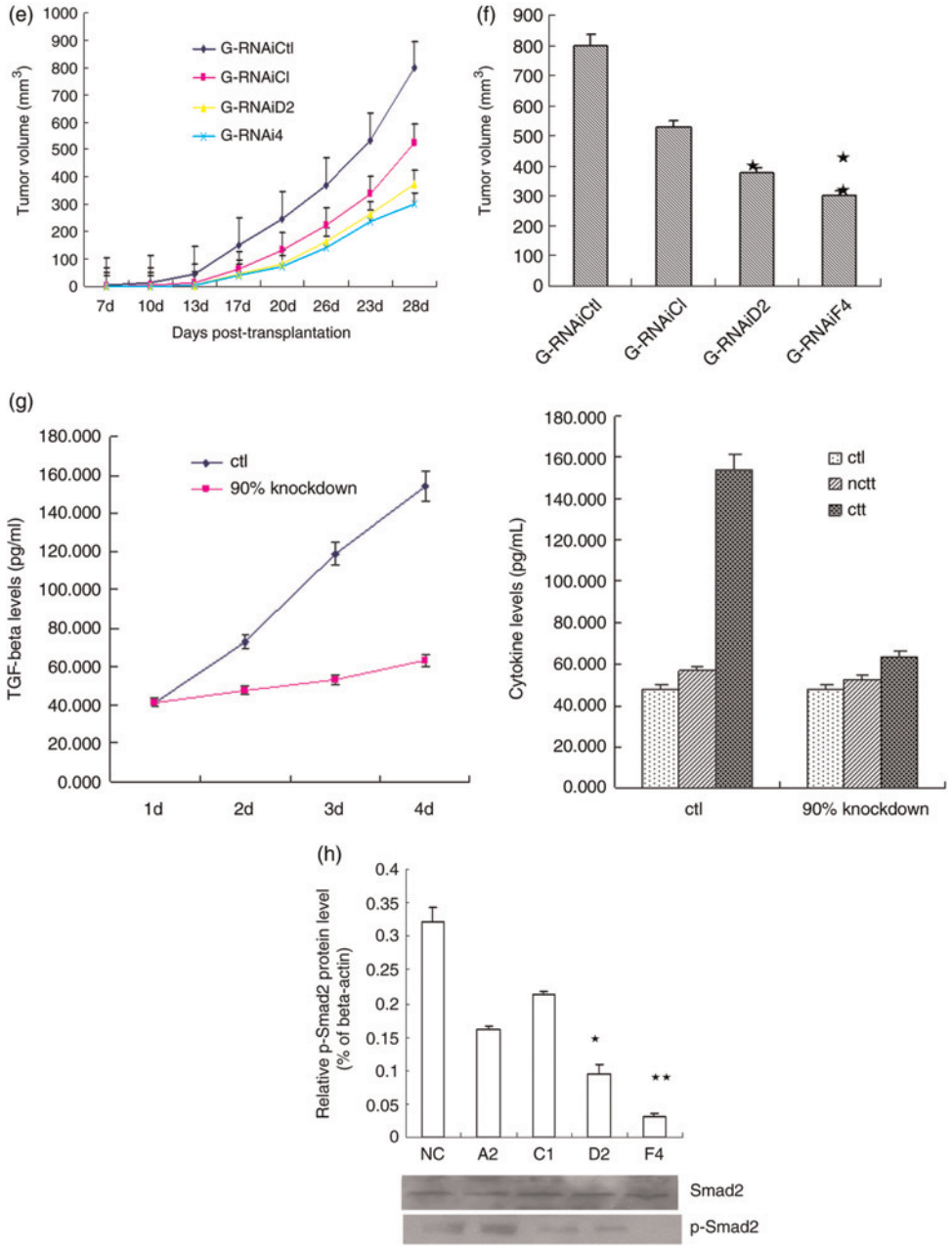

Figure 4 Continued

postulated to be mediated by both paracrine effects in the local tumor–stromal environment, including the effects of TGF-β1 on immune surveillance, angiogenesis and increased tumor interstitial pressure, as well as autocrine effects inducing survival signals directly in tumor cells.[40,41] Several studies have now shown the antitumor effects of inhibiting the TGF-β1 pathway.[35,38,39,42,43] In support of the idea, we found malignant transformation of the hEpSCs mediated by the local activation of TGF-β1/Smad signaling pathways.

Integrins, cell-surface receptors that mediate adhesive interactions between cells and the extracellular matrix, play an important role in cancer progression.[44] ITGAV subunit heterodimerizes with five different β subunits, and at least three of these integrins, $\alpha v\beta 1$, $\alpha v\beta 5$ and $\alpha v\beta 6$, are expressed at varying levels in normal and malignant epithelial cells of the skin.[45] The M21-L human melanoma cell line, lacking $\alpha v\beta 3$ integrin expression, has a dramatically reduced ability to induce tumors and metastases in nude mice. Expression of $\alpha v\beta 3$ in M21-L cells restored their tumorigenic properties.[46] Furthermore, subcutaneous growth of $\alpha v\beta 3$-positive M21 melanoma cells in nude mice was reduced significantly by αv-specific blocking antibodies.[47] Prior studies showed that alpha v integrins have been shown to promote tumor growth through regulating caspase activity and hence cell survival.[48–50] Recently, He *et al.*[51] showed that down-regulation of alpha v integrin by retroviral delivery of small interfering siRNA significantly reduced drug resistance of HT29 multicellular spheroids and HT29 xenografts *in vivo*. Van Aarsen *et al.*[52]

suggested antibody-mediated blockade of the $\alpha v\beta 6$ receptor inhibits tumor progression *in vivo* via a mechanism that involves TGF-β. The $\alpha v\beta 6$ can bind to TGF-$\beta 1$ and TGF-$\beta 3$ and lead to local activation of TGF-β, which in turn may affect the neighboring cells in a paracrine fashion.[53] These data are consistent with our results that ITGAV may contribute to the tumorigenesis and mediate the local activation of TGF-$\beta 1$/Smad signaling pathways.

In conclusion, the microenvironment created by melanoma cells can lead to cancer formation of latent neoplastic SCs. Such a microenvironment is a necessary condition for the carcinogen DMBA to convert hEpSCs to melanoma cells. Direct contact between tumor cells and SCs, which causes the local activation of TGF-$\beta 1$/Smad signaling pathways via ITGAV, is essential to malignant transformation. Better understanding the molecular mechanisms by which melanoma cells exert these effects may open up new venues for cancer therapeutic and preventive interventions.

Author contributions: HS performed all the experiments, contributed to the interpretation of the results and drafted the manuscript. KH participated in the design of the study, performed the statistical analysis and contributed to data interpretation. MW isolated hEpSCs and examined the hEpSCs. JX and LY contributed to the experimental design, to the interpretation of the results and to the writing up of the manuscript. YT and YY undertook the confocal photographs. HL conceived the study, contributed to the experimental design, supervised the acquisition of data and the analysis of the data, and contributed to the interpretation of the results and to the writing up of the manuscript. All authors read and approved the final version of the manuscript.

ACKNOWLEDGEMENTS

This work was supported by the Natural Science Foundation of China General Program (No. 30870511).

REFERENCES

1 Soto AM, Sonnenschein C. The somatic mutation theory of cancer: growing problems with the paradigm? *BioEssays* 2004;**26**:1097–107
2 Weaver VM, Gilbert P. Watch thy neighbor: cancer is a communal affair. *J Cell Sci* 2004;**117**:1287–90
3 Osawa M, Hanada K, Hamada H, Nakauchi H. Long-term lymphohematopoietic reconstitution by a single CD34-low/negative hematopoietic stem cell. *Science* 2006;**273**:242–5
4 Reynolds BA, Weiss S. Clonal and population analyses demonstrate that an EGF-responsive mammalian embryonic CNS precursor is a stem cell. *Dev Biol* 1996;**175**:1–13
5 Kim CF, Jackson EL, Woolfenden AE, Lawrence S, Babar I, Vogel S, Crowley D, Bronson RT, Jacks T. Identification of bronchioalveolar stem cells in normal lung and lung cancer. *Cell* 2005;**121**:823–35
6 Lam JS, Reiter RE. Stem cells in prostate and prostate cancer development. *Urol Oncol* 2006;**24**:131–40
7 Allinen M, Beroukhim R, Cai L, Brennan C, Lahti-Domenici J, Huang H, Porter D, Chin L, Richardson A, Schnitt S, Sellers WR, Polyak K. Molecular characterization of the tumor microenvironment in breast cancer. *Cancer Cell* 2004;**6**:17–32
8 Bissell MJ, LaBarge MA. Context, tissue plasticity, and cancer: are tumor stem cells also regulated by the microenvironment? *Cancer Cell* 2005;**7**:17–23
9 Tang C, Ang BT, Pervaiz S. Cancer stem cell: target for anti-cancer therapy. *FASEB J* 2007;**21**:3777–85
10 Vogelstein B, Kinzler KW. The multistep nature of cancer. *Trends Genet* 1993;**9**:138–41
11 Calabrese P, Tavare S, Shibata D. Pretumor progression: clonal evolution of human stem cell populations. *Am J Pathol* 2004;**164**:1337–46
12 Li L, Xie T. Stem cell niche: structure and function. *Annu Rev Cell Dev Biol* 2005;**21**:605–31
13 Kim KM, Calabrese P, Tavare S, Shibata D. Enhanced stem cell survival in familial adenomatous polyposis. *Am J Pathol* 2004;**164**:1369–77
14 Gao JX. Cancer stem cells: the lessons from precancerous stem cells. *J Cell Mol Med* 2008;**12**:67–96
15 Rubin H. Microenvironmental regulation of the initiated cell. *Adv Cancer Res* 2003;**90**:1–62
16 Bhowmick Neilson EG, Moses HL. Stromal fibroblasts in cancer initiation and progression. *Nature* 2004;**432**:332–7
17 Kuperwasser T, Chavarria M, Magrane G, Gray JW, Carey L, Richardson A, Weinberg RA. Reconstruction of functionally normal and malignant human breast tissues in mice. *Proc Natl Acad Sci USA* 2004;**101**:4966–71
18 Olumi AF, Grossfeld GD, Hayward SW, Carroll PR, Tlsty TD, Cunha GR. Carcinoma-associated fibroblasts direct tumor progression of initiated human prostatic epithelium. *Cancer Res* 1999;**59**:5002–11
19 Abbott DE, Bailey CM, Postovit LM, Seftor EA, Margaryan N, Seftor RE, Hendrix MJ. The epigenetic influence of tumor and embryonic microenvironments: how different are they? *Cancer Microenviron* 2008;**1**:13–21
20 Postovit LM, Seftor EA, Seftor REB, Hendrix MJC. A 3-D model to study the epigenetic effects induced by the microenvironment of human embryonic stem cells. *Stem Cells* 2006;**24**:501–5
21 Seftor EA, Brown KM, Chin L, Kirschmann DA, Wheaton WW, Protopopov A, Feng B, Balagurunathan Y, Trent JM, Nickoloff BJ, Seftor RE, Hendrix MJ. Epigenetic transdifferentiation of normal melanocytes by a metastatic melanoma microenvironment. *Cancer Res* 2005;**65**:10164–9
22 Zhou JX, Chen SY, Liu WM, Cao YJ, Duan EK, Enrichment and identification of human 'fetal' epidermal stem cells. *Hum Reprod* 2004;**19**:968–74
23 Jones PH, Watt FM. Separation of human epidermal stem cells from transit amplifying cells on the basis of differences in integrin function and expression. *Cell* 1993;**73**:713–24
24 Kopper L, Hajdu M. Tumor stem cells. *Pathol Oncol Res* 2004;**10**:69–74
25 Kang Y, Massague A. Epithelial–mesenchymal transitions: twist in development and metastasis. *Cell* 2004;**118**:277–9
26 Maeda M, Johnson KR, Wheelock MJ. Cadherin switching: essential for behavioral but not morphological changes during an epithelium-to-mesenchyme transition. *J Cell Sci* 2005;**118**:873–87
27 Bates RC, Mercurio AM. The epithelial–mesenchymal transition (EMT) and colorectal cancer progression. *Cancer Biol Ther* 2005;**4**: 365–70
28 Zeisberg M, Maeshima Y, Mosterman B, Kalluri R. Extracellular matrix microenvironment regulates migratory behavior of activated tubular epithelial cells. *Am J Pathol* 2002;**160**:2001–8
29 Thiery JP. Epithelial–mesenchymal transitions in development and pathologies. *Curr Opin Cell Biol* 2003;**15**:740–6
30 Valdes F, Alvarez AM, Locascio A. The epithelial mesenchymal transition confers resistance to the apoptotic effects of transforming growth factor Beta in fetal rat hepatocytes. *Mol Cancer Res* 2002;**1**: 68–78
31 Kleeff J, Ishiwata-Maruyama H, Friess H, Truong P, Büchler MW, Falb D, Korc M. The TGF-beta signaling inhibitor Smad7 enhances tumorigenicity in pancreatic cancel. *Oncogene* 1999;**18**:5363–72
32 Gorelik L, Flavell RA. Eradication of tumors through the blockade of transforming growth factor-beta signaling in TGF-beta. *Nat Med* 2001;**7**:1118–22
33 Chen W, Wahl SM. TGF-β: receptors, signaling pathways and autoimmunity. In: Altman A, ed. *Signal Transduction Pathways in Autoimmunity. Curr Dir Autoimmun* 2002;**5**:62–91
34 Li MO, Wan YY, Sanjabi S, Robertson AK, Flavell RA. Transforming growth factor-β regulation of immune responses. *Annu Rev Immunol* 2006;**24**:99–146
35 Yingling JM, Blanchard KL, Sawyer JS. Development of TGF-β signalling inhibitors for cancer. *Nat Rev Drug Discov* 2004;**3**:1011–22

36 Bierie B, Moses HL. Tumor microenvironment: TGF-β: the molecular Jekyll and Hyde of cancer. *Nat Rev Cancer* 2006;**6**:506–20
37 Akhurst RJ, Derynk R. TGF-β signaling in cancer-a double-edged sword. *Trends Cell Biol* 2001;**11**:S44–51
38 Muraoka RS, Dumont N, Ritter CA, Dugger TC, Brantley DM, Chen J, Roebuck LR, Ryan S, Gotwals PJ, Koteliansky V, Arteaga CL. Blockade of TGF-β inhibits mammary tumor cell viability, migration, and metastasis. *J Clin Invest* 2002;**109**:1551–9
39 Yang YA, Dukhanina O, Tang B, Mamura M, Letterio JJ, MacGregor J, Patel SC, Khozin S, Liu ZY, Green J, Anver MR, Merlino G, Wakefield LM. Lifetime exposure to a soluble TGF-β antagonist protects mice against metastasis without adverse side effects. *J Clin Invest* 2002;**109**:1607–15
40 Muraoka-Cook RS, Shin I, Yi JY, Easterly E, Barcellos-Hoff MH, Yingling JM, Zent R, Arteaga CL. Activated type I TGF-β receptor kinase enhances the survival of mammary epithelial cells and accelerates tumor progression. *Oncogene* 2006;**25**:3408–23
41 Ao M, Williams K, Bhowmick NA, Hayward SW. Transforming growth factor-{β} promotes invasion in tumorigenic but not in nontumorigenic human prostatic epithelial cells. *Cancer Res* 2006;**66**:8007–16
42 Halder SK, Beauchamp RD, Datta PK. A specific inhibitor of TGF-β receptor kinase, SB-431542, as a potent antitumor agent for human cancers. *Neoplasia* 2005;**7**:509–21
43 Akhurst RJ. Large- and small-molecule inhibitors of transforming growth factor-β signaling. *Curr Opin Invest Drugs* 2006;**7**:513–21
44 McCarty JH, Barry M, Crowley D, Bronson RT, Lacy-Hulbert A, Hynes RO. Genetic ablation of αv integrins in epithelial cells of the eyelid skin and conjunctiva leads to squamous cell carcinoma. *Am J Pathol* 2008;**172**:1740–7
45 Watt FM. Role of integrins in regulating epidermal adhesion, growth and differentiation. *EMBO J* 2002;**21**:3919–26
46 Felding-Habermann B, Mueller BM, Romerdahl CA, Cheresh DA. Involvement of integrin alpha V gene expression in human melanoma tumorigenicity. *J Clin Invest* 1992;**89**:2018–22
47 Mitjans F, Sander D, Adán J, Sutter A, Martinez JM, Jäggle CS, Moyano JM, Kreysch HG, Piulats J, Goodman SL. An anti-αv-integrin antibody that blocks integrin function inhibits the development of a human melanoma in nude mice. *J Cell Sci* 1995;**108**:2825–38
48 Petitclerc E, Strömblad S, von Schalscha TL, Mitjans F, Piulats J, Montgomery AM, Cheresh DA, Brooks PC. Integrin alpha(v)beta3 promotes M21 melanoma growth in human skin by regulating tumor cell survival. *Cancer Res* 1999;**11**:2724–30
49 Stupack DG, Puente XS, Boutsaboualoy S, Storgard CM, Cheresh DA. Apoptosis of adherent cells by recruitment of caspase-8 to unligated integrins. *J Cell Biol* 2001;**3**:459–70
50 Stupack DG, Teitz T, Potter MD, Mikolon D, Houghton PJ, Kidd VJ, Lahti JM, Cheresh DA. Potentiation of neuroblastoma metastasis by loss of caspase-8. *Nature* 2006;**7072**:95–9
51 He J-M, Wang F-C, Qi H-B, Li Y, Liang H-J. Down-regulation of αv integrin by retroviral delivery of small interfering RNA reduces multicellular resistance of HT29. *Cancer Lett* 2009;**284**:182–8
52 Van Aarsen LA, Leone DR, Ho S, Dolinski BM, McCoon PE, LePage DJ, Kelly R, Heaney G, Rayhorn P, Reid C, Simon KJ, Horan GS, Tao N, Gardner HA, Skelly MM, Gown AM, Thomas GJ, Weinreb PH, Fawell SE, Violette SM. Antibody-mediated blockade of integrin alpha v beta 6 inhibits tumor progression *in vivo* by a transforming growth factor-beta-regulated mechanism. *Cancer Res* 2008;**68**:561–70
53 Munger JS, Huang X, Kawakatsu H, Griffiths MJ, Dalton SL, Wu J, Pittet JF, Kaminski N, Garat C, Matthay MA, Rifkin DB, Sheppard D. The integrin $\alpha v\beta 6$ binds and activates latent TGFβ1: a mechanism for regul ating pulmonary inflammation and fibrosis. *Cell* 1999;**96**:319–28

(Received March 29, 2010, Accepted November 23, 2010)